Chinese Chemical Letters 33 (2022) 2231–2242

Contents lists available at ScienceDirect

Chinese Chemical Letters

journal homepage: www.elsevier.com/locate/cclet

An integrative review on the applications of 3D printing in the field of *in vitro* diagnostics

Jian Yang[a,1], Yanxiang Cheng[a,1], Xia Gong[a], Shengzhu Yi[a], Cheuk-Wing Li[c], Lelun Jiang[a,*], Changqing Yi[a,b,*]

[a] *Guangdong Provincial Key Laboratory of Sensor Technology and Biomedical Instrument, School of Biomedical Engineering, Sun Yat-sen University, Shenzhen 518107, China*
[b] *Research Institute of Sun Yat-sen University in Shenzhen, Shenzhen 518057, China*
[c] *School of Science and Technology, Nottingham Trent University, Clifton Lane, Nottingham NG11 8NS, United Kingdom*

ARTICLE INFO

Article history:
Received 8 July 2021
Revised 3 August 2021
Accepted 23 August 2021
Available online 28 August 2021

Keywords:
3D printing
In vitro diagnostics
Portable sensing device
Point-of-care testing
Stereolithography (SLA)
Digital light projection (DLP)
Fused deposition modeling (FDM)

ABSTRACT

Biomedicine is one of the fastest growing areas of additive manufacturing. Especially, in the field of *in vitro* diagnostics (IVD), contributions of 3D printing include i) rapid prototyping and iterative IVD proof-of-concept designing ranging from materials, devices to system integration; ii) conceptual design simplification and improved practicality of IVD products; iii) shifting the IVD applications from centralized labs to point-of-care testing (POCT). In this review, the latest developments of 3D printing and its advantages in IVD applications are summarized. A series of 3D-printed objects for IVD applications, including single-function modules, multi-function devices which integrate several single-function modules for specific analytical applications such as sample pre-treatment and chemo-/bio-sensing, and all-in-one systems which integrate multi-function devices and the instrument operating them, are analyzed from the perspective of functional integration. The current and potential commercial applications of 3D-printed objects in the IVD field are highlighted. The features of 3D printing, especially rapid prototyping and low start-up, enable the easy fabrication of bespoke modules, devices and systems for a range of analytical applications, and broadens the commercial IVD prospects.

1. Introduction

1.1. Significance of IVD

In vitro diagnostics (IVD) which refers to diagnostic tests performed outside the human body, is essential for the healthcare system in diagnosing disease, preventing infections, managing chronic disease, tracking pathological changes, evaluating therapeutic effects, and beyond [1-7]. According to the Food and Drug Administration (FDA), IVD products include the diagnostic reagents, instruments, and integrated systems intended for the collection, preparation, and analysis of samples such as blood, interstitial fluid (ISF), urine, sweat, saliva, and tissues. Since some analytes in blood can permeate into ISF, saliva, and sweat, a good correlation can always be found between their concentrations in blood and those in ISF, saliva or sweat [8]. Integrated with typical detection strategies such as colorimetric, electrochemical, and fluorescent methods, IVD products can offer economical and personalized healthcare to end users. IVD tests have many distinct features in clinical care [7-9]: IVD tests do not require direct contact with the human body, thus avoiding possible biosafety concerns of *in vivo* test; IVD tests are often minimally invasive or non-invasive; IVD tests can facilitate early diagnosis of disease, thus reducing the cost of extensive treatment; IVD products often serve on the front lines of saving human lives and improving healthcare services, for example, the prevention of infectious diseases such as coronavirus disease 2019 (COVID-19), and chronic disease management such as homecare for diabetes.

1.2. Challenges of IVD

Remarkable achievements have been made in IVD during the last few decades, and the global IVD market size is expected to reach 74.46 billion dollars by 2022 [10]. Despite the rapid growth, limitations and challenges still exist in IVD: i) automation and the integration with general workflows; ii) miniaturization and afford-

* Corresponding authors.
E-mail addresses: jianglel@mail.sysu.edu.cn (L. Jiang), yichq@mail.sysu.edu.cn (C. Yi).
[1] These authors contributed equally to this work.

https://doi.org/10.1016/j.cclet.2021.08.105
1001-8417/

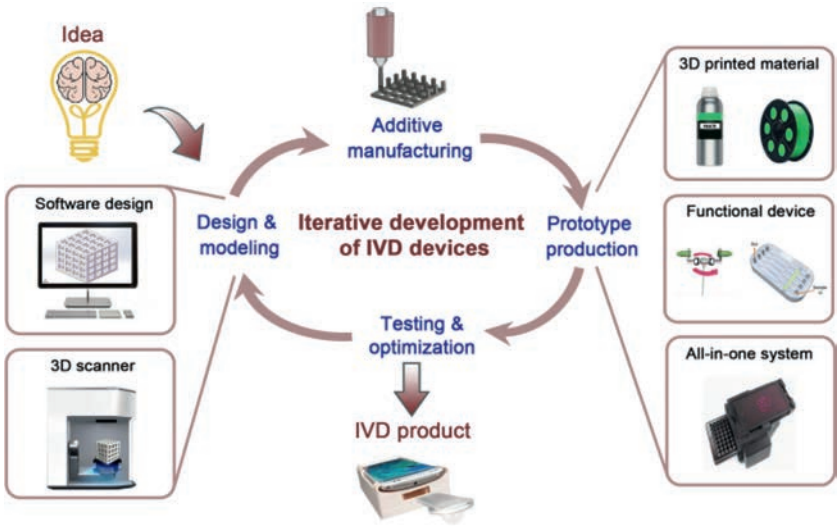

Fig. 1. Typical iterative development process of 3D-printed IVD products. The iterative development process of customized IVD products includes 3D modeling and design, 3D printing (additive manufacturing), prototyping, testing, and optimization. The prototype productions of IVD refer to 3D printed resign, functional device to all-in-one system. The image of IVD product is downloaded from the network (https://consumer.healthday.com/infertility-information-22/infertility-news-412/smartphone-device-sizes-up-sperm-health-720902.html).

ability; iii) the manufacture precision of complex IVD devices and instruments. Fortunately, 3D printing, a cost-effective, rapid, and precision manufacturing technology, is emerging to meet these demands.

MobileODT, for example, adopted 3D printing to manufacture customized substrate holders tailored for mobile phones and created a portable testing instrument that takes photos of the cervix and enlarges the images to help doctors diagnose cervical cancer. More importantly, the cost of MobileODT's 3D-printed device is $\sim$ $1,500, only a tenth of the conventional magnification device, making it ideal for cervical cancer screening in third world countries that lack specialized medical facilities. This example clearly illustrates that 3D printing reduces the financial and time cost of prototyping and producing IVD products, and offers rapid transfer from centralized tests to decentralized tests.

1.3. 3D printing for IVD

3D printing has become a robust tool for fabricating a large variety of analytical devices in the past few years, and has brought significant advancements in the IVD field [1,11-16]. One of the most favorable features of 3D printing is unarguably the direct design-to-object workflow that facilitates the one-step fast prototyping of devices with complex geometry and the iterative design of proof-of-concept IVD devices [17-21]. For example, with precision manufacture, 3D printing contributes to manufacturing multi-function microfluidic devices with sophisticated internal microstructures in a single step, making the devices profoundly effective in specific analytical stages of IVD tests, such as sample pretreatment, reagent mixing, as well as quantitation [22]. With these intrinsically advantageous properties, 3D printing is proven to be beneficial in the complete IVD device development workflow, from conceptualization, design to testing and optimization of the functional prototype (Fig. 1).

Point-of-care testing (POCT) is now a continuously expanding trend in the practice of IVD [17]. POCT can fulfil a critical need in the modern healthcare ecosystem, because they are designed for performing diagnostic tests outside central or decentralized laboratories. The advantages of POCT include short testing time, fast results, limited sample degradation, unrestricted space, more frequent testing, and simple operation that can even be performed by non-professionals. These advantages enable that clinical management decisions can be made quickly and result in improved patient safety and clinical outcomes. However, the current development pipeline for POCT products is highly bottlenecked due to the restraints in material, cost, and manufacture techniques. Fortunately, 3D printing allows for a more affordable and faster process to a working prototype than conventional manufacture techniques, thus facilitating the research and development of POCT technology. Obviously, 3D printing technology will play a continuously growing role in shift of IVD tests from centralized labs to point-of-care through facile and cost-effective manufacturing of portable POCT instruments.

Considering that the function integration levels of the 3D-printed IVD products vary from single-function modules to all-in-one systems, it is necessary to review the research progress in this field. In this context, the current study discussed the advantages of 3D printing for IVD applications. After a brief and concise overview of 3D printing for IVD product development, typical examples of 3D-printed products for IVD tests were summarized and categorized. In addition, comprehensive coverage of current and potential future commercial 3D-printed IVD products were categorized from key components and accessories to instruments. Finally, the conclusions and the outlooks of 3D printing in IVD field are outlined.

2. Overview of 3D printing in IVD

2.1. Typical iteration development workflow for IVD

Although the IVD industry is snowballing in recent years, the Research and Development of IVD products is still severely bottlenecked due to the high cost and complexity of traditional manufacturing processes [19,23,24]. As the development of cheap, simple but effective IVD products is highly desirable for healthcare systems, it is important to understand how an IVD product is translated from lab to market [24]. The iterative design-built-testing cycles are crucial for IVD product development from conceptualization to prototyping, as shown in Fig. 1. The typical iterative development process of a customized IVD product includes 3D modeling and design, 3D printing, prototyping, testing, and optimization.

When an original IVD product concept or an idea emerges, a 3D model is designed, then the prototype is 3D-printed based on the designed model, and finally, the prototype is tested and optimized. Once the design-to-object iterative development of a prototype is verified in the lab, the development pipeline shifts to industrial research.

More specifically, the iterative development of IVD begins with establishing a 3D model using computer-aided design (CAD) software or a 3D scanner. The CAD model file is then converted into an STL file, sliced into a series of cross-sectional layers, and the G-codes are generated for the 3D printer [23,25-27]. The key parameters of the 3D printing process (such as printing path, printing speed, and layer height) are controlled *via* G-codes [28]. The prototype is fabricated by layer-by-layer deposition of materials from bottom to top, forming the target object from 2D to 3D [27,29]. With the development of 3D printing in terms of printing size, accuracy, and complexity, IVD prototypes can be rapidly produced through 3D printing. The 3D-printed IVD prototypes include single-function modules, multi-functional devices and all-in-one systems. It is worthy to mention that 3D printing can play a role in interfacing the device and housing the electronics and supporting hardware, but it is rare the whole instrument is manufactured by 3D printing. These tools or devices are repeatedly tested and optimized on-site or in labs. The IVD prototypes gradually reach clinical requirements through several generations of interactive development.

2.2. The 3D printing techniques for IVD

The 3D printing technology is a family of flexible additive manufacturing techniques that enable rapid and accurate fabrication of complex 3D structures. The various 3D printing techniques differ in the ways that raw materials are bonded together [30,31]. Some typical 3D printing techniques, such as stereolithography (SLA), digital light projection (DLP), fused deposition modeling (FDM), and inkjet printing, are usually applied in the IVD field [32-37]. The other printing techniques, such as aerosol jetting, laser selective melting, powder bed fusion, and laminated object manufacturing, are rarely used in the production of IVD prototypes, therefore not discussed in this review.

SLA utilizes movable ultraviolet (UV) light or laser beam to selectively cure a working surface submerged in a container of liquid photosensitive resin into a solidified layer. Immersing this layer in a controlled manner enables the successive layer to be solidified and stacked on the previous layer with good adhesion. Each 2D layer solidifies and melds into the previous layers, finally forming a 3D object [13,30,38,39]. The resolution of SLA is mainly determined by the diameter of the light beam and the absorption properties of photosensitive resin. Kadimisetty *et al.* [30] employed an SLA 3D printer to produce compact plastic arrays whose internal chambers could store assay reagents, samples, and detection chips for the immunoassays of multiple proteins. The use of 3D printing made it possible for the mass production of disposable microfluidic devices with optimized design features. Material Jetting (MJ) is one of the fastest and most accurate 3D printing techniques. Its working mechanism is to print products by spraying and solidifying liquid photopolymer droplets under UV light. MJ is similar to SLA in that UV light is employed to cure the resin. The difference is that the MJ 3D printer sprays hundreds of tiny droplets at one time, while the SLA 3D printer selectively cures the photosensitive resin point-by-point with a laser.

Recently, a more advanced DLP 3D printing technique was developed [13], in which the digital light source projects on the surface of the liquid photosensitive resin and cures an entire layer of resin at one time. Each layer is projected as a 2D image produced by digitally sectioning the 3D object into thin slices. Thereby, the printing speed is effectively improved in comparison with the traditional SLA technique. The resolution of DLP mainly depends on the size of the projected pixel. It should also be noted that the z resolution of DLP is as much influenced by the resin as it is by the printers z resolution of the stage. The key component of DLP is the digital micromirror device. The cost of DLP 3D printers has been significantly reduced due to the advent of inexpensive digital micromirror devices and commercially available projectors. For instance, Stassi *et al.* [40] adopted the DLP technique to fabricate arrays of microcantilevers with complex 3D microstructure for biosensing applications.

In addition, liquid crystal display (LCD) and DLP 3D printing technologies are quite similar, but the main difference exists in the light source to cure photopolymer resins. Actually, LCD printers have found a rapid increase in market share. For LCD printing, the UV light transports through the LCD displayer, as a mask, thereby selectively projects on the surface of the liquid photosensitive resin and cures it. As a cost-effective and mass manufacturing technique, LCD 3D printing focuses on big and detailed functional parts. Though rarely applied in IVD field at this stage, it is believed that LCD printing might play a growing role in IVD field in the near future.

For the record, the printed materials of SLA and DLP are mostly photocrosslinkable resins, because the selection of 3D printing materials for IVD is limited due to light transmittance, biocompatibility, mechanical properties, surface property, and resolution. Photosensitive polymers are synthesized with monomers, oligomers, and photoinitiators. The typical 3D printing resins include acrylic-based resins, epoxy resins, and mixed resins such as urethane acrylate, poly(ethylene glycol) diacrylate, poly(methyl methacrylate), polypropylene fumarate, and poly(D, L-lactide). Photopolymers often have high optical transparency, and excellent precision.

FDM is the most used 3D printing technique in academic labs. FDM-printed objects are created by heating and melting various hot-melt filamentous materials [23]. After being heated to a semi-flow state, the thermoplastic polymer is extruded from the nozzle and deposited on the previous layer. Next, the thermoplastic polymer is cooled and melded into the previous layers. The nozzle is then raised to complete the next layer deposition till the whole 3D object is fabricated. Recently, Cardoso *et al.* [39] employed FDM to directly print graphene or polylactic acid electrodes and constructed amperometric biosensors to detect glucose, nitrite, and uric acid in blood plasma, saliva, and urine, respectively. With FDM 3D printers, the printing materials are thermoplastics [41-45]. Typical thermoplastic materials include polycaprolactone, polylactic acid, polylactic acid-glycolic acid, polybutylene terephthalate, polystyrene, polycarbonate, and polyethylene terephthalate acrylonitrile butadiene styrene (ABS). These thermoplastic raw materials are easy to store, transport, process, and only rely on high-temperature molding. The manufacturing process only requires limited chemical or mechanical post-processing to remove loose threads and sometimes enhance appearance. In a word, FDM technology is easy to use in the laboratory, thanks to its characteristics such as low manufacturing cost and diversified raw materials.

Inkjet printing includes continuous inkjet and drop-on-demand systems. The ink droplets are continuous or drop-by-drop ejected on the substrate using the thermosensitive or piezoelectric nozzle. These droplets deposited on the substrate in a predesigned pattern will be solidified by light or heat. The 3D object is built by repeating the spraying and curing process [46,47]. Fontes *et al.* [46] inkjet printed the capture and detection antibodies on the hybrid zwitterionic brush for a point-of-care sandwich immunoassay. The photopolymer material for inkjet printing is similar to the materials used in the SLA process. Inkjet printing materials mainly contain polymer ink, nano-silver ink, graphene ink, and bio-ink. Furthermore, the multi jet modeling process in inkjet printing also uses

Table 1
Typical 3D printing techniques for IVD.

3D printings	SLA	DLP	FDM	Polymer inkjet printing
Illustrations	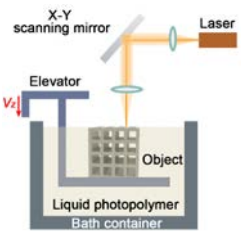	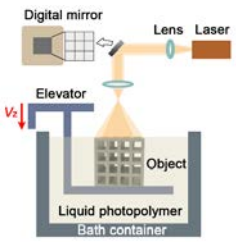	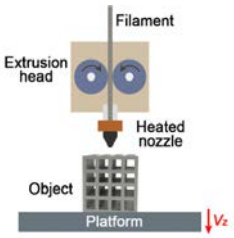	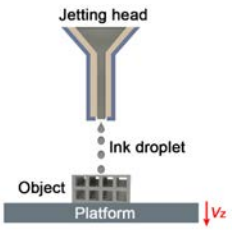
Materials	Liquid photocurable resins	Liquid photocurable resins	Thermoplastic filamentous polymers	Polymer or bioactive material
Advantages	High Z and X-Y resolution (25 and 30-150 μm, respectively) [20], high quality, no printing size limitation	High Z and X-Y resolution (25 and 30-150 μm, respectively) [20], rapid printing;	Low cost, simple manufacturing	High X-Y resolution (25-80 μm) [20], rapid printing, no printing size limitation
Limitations	Material constraint, slow printing, relative expensive	Material constraint, limited printing size	Low Z and X-Y resolution (> 100 μm and 100–400 μm, respectively) [20], material constraint (only thermoplastics), affected by temperature	Medium Z resolution (70-120 μm) [20], lack of interlaminar adhesion
IVD Applications	Bionic tissue [48], Microfluidic array [30,49], Microfluidic chip [34,50]	Biosensor [51], hydrogel microneedles [28]	Electrochemical detection platform [52]; electrode [53], auxiliary device [29]	Finger-actuated pump detector [46], flow cell [9]

Notes: stereolithography (SLA), digital light projection (DLP), fused deposition modeling (FDM).

sacrificial support materials such as water-soluble gel-like materials or meltable waxes.

The above-mentioned 3D printing techniques are described in detail, and the key features of the four techniques, including the materials, advantages, and limitations, are summarized, as listed in Table 1 [48-53]. For better comparison of the these 3D printing techniques for IVD applications, the representative analytical performance of the selected 3D-printed IVD products is highlighted in Table 2 [54-57]. As can be seen, 3D printing technology is suitable for the manufacture of IVD products ranging from single-function modules to multi-functional devices.

2.3. Advantages and limitations of 3D printing in the field of IVD

The main advantages of 3D printing IVD prototypes over traditional technologies are manifested in the customization of complex 3D geometry, simplification of the production process, and reduction of cost [58]:

(1) Customization of complex 3D geometry. The major bottleneck for traditional subtractive manufacturing is the construction of freeform 3D structures. Conversely, prototypes with complex 3D geometry could be easily designed and constructed using a layer-by-layer deposition since 3D printing is an additive manufacturing process. Customized fabrication of IVD products *via* 3D printing only requires simple operational protocols yet allows rapid reproduction. These benefits are very evident as compare to industrial manufacturing methods.

(2) Simplification of the fabrication process for working prototypes. The 3D printing technology simplifies the production process of prototypes as the mold manufacture and assembly steps are not required. Furthermore, the 3D printing technology shortens the manufacturing time to hours or minutes instead of days or months with traditional methods. The printing time is naturally determined by the size and complexity of the model as well as the performance of the printer. Importantly, 3D printing speeds up the entire iteration process with frequent minor changes to the prototype.

(3) Reduction of the cost (material, energy, time, and training). The traditional mechanical processing methods often require expensive machinery with large energy consumption [59-61]. The 3D printing technology reduces the energy costs and the waste of raw materials and eliminates the need for professional operation, guidance, technical personnel, and the cooperation of workshop assembly lines. Especially, 3D printing is very well suited for those small to medium sized jobs that may require a lot of customization. The 3D printing technology only requires mastering the related software and the 3D printer. Therefore, 3D printing greatly reduces the costs of human resources and materials.

Although the application of 3D printing has narrowed the gap between academic research and industrial manufacture, there are still some limitations. For example, (1) the scope of printing materials is too small to fully satisfy the requirements of industrial production, making it difficult to up-scale and generalize the 3D printing technology; 2) the 3D-printed objects are not as good as the integrally casted ones in many aspects such as strength, stiffness, and fatigue resistance because of the layer-by-layer manufacturing process.

3. The 3D-printed IVD products

IVD products often feature specialized components and elements to meet various analytical requirements [34-37,40,62-65]. The recent advance of 3D printing in the fabrication of IVD products was reviewed. To portray a systematic overview of the field, 3D-printed devices were categorized into single-function modules, multi-function devices which integrate several single-function modules for specific analytical applications such as sample pretreatment and chemo-/bio-sensing, and all-in-one sensing systems which integrate multi-function devices and the instrument operating them, according to the level of function integration.

Table 2
A summary of the representative analytical features of 3D-printed IVD devices.

3D printing techniques	IVD devices	3D-printed components	Raw materials	Analytes	Detection range	LODs	CV	Samples	Refs.
SLA	Blood viscosity analysis platform	 Capillary circuit	Acrylate-based photopolymer resin	Blood viscosity	4.8-71.2 cP	-	8.3%	Blood	[37]
	Handheld spectrometer	Housing 	Acrylate-based photopolymer resin	Hemoglobin	19-192 mg/mL	2.31 mg/mL	< 1.23%	Blood	[54]
DLP	3D, paper-based microfluidic analytical device	Support 	ACRYL-3DK83W	Glucose, cholesterol and triglyceride	Glucose 5-11 mmol/L, Cholesterol 2.6-6.7 mmol/L, Triglyceride 1-2.3 mmol/L	Glucose 0.3 mmol/L, Cholesterol 0.2 mmol/L, Triglyceride 0.3 mmol/L	< 9%	Serum	[55]
FDM	Electrochemical chip	Transparent miniature cell and vessel 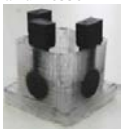	PLA and carbon-loaded acrylonitrile butadiene styrene	Paracetamol and caffeine	0-22.5 mg/L	Paracetamol 0.43 mg/L, Caffeine 0.39 mg/L	Paracetamol 7.6%, Caffeine 4.8%	phosphate buffer	[56]
	Electrochemical biosensor	Working electrode	PLA/graphene	Glucose, uric acid and nitrite,	Glucose 0.5-6.5 mmol/L, Uric acid 0.5-250 μmol/L, Nitrite 0.5-250 μmol/L	Glucose 15 μmol/L; Uric acid 0.02 μmol/L, Nitrite 0.03 μmol/L	Glucose < 5%, Uric acid 2.1%, Nitrite 1.1%	Plasma and BR buffer,	[39]
Inkjet printing	Circulating tumor cells isolation platform	Microfluidic channel	Photoplastic build material and wax support material	Circulating tumor cells	-	Efficiencies more than 87.74%	-	Blood	[57]

3.1. Single-functional modules

3.1.1. Simple IVD tools

The representatives of 3D printing in the field of IVD are simple tools to fulfill critical needs such as mold, pump, support, and fluidic manipulation (mixing, separation, reaction). For example, Barber *et al.* [36] introduced 3D-printed molds to replicate polydimethylsiloxane (PDMS)-based microfluidic chips (Fig. 2A). The 3D-printed microfluidic chip, which is fabricated from wax with Multi Jet Fusion technology, overcomes the typical microfabrication bottlenecks: complex photolithography and expensive specialized equipment. In addition to 3D-printed molds, an open-source peristaltic pump that can process small volume point-of-care (POC) liquid has been demonstrated by combining 3D-printed parts and an Arduino microcontroller, which is amenable to small volume POC liquid handling [35]. All 3D-printed parts were printed by ABS plastic with an SLA photo-curing 3D-printer. The low-cost (∼ $120) 3D-printed peristaltic pump enabled not only customized flow profiles to fit requirements of processing low volume liquid but also control flow rate precisely up to 1.6 mL/min (Fig. 2B). In another study, a smartphone mountable low-power 3D-printed fan has been successfully exploited as a portable centrifuge system for separating functionalized magnetic particles and Sepharose (Fig. 2C) [63]. The handheld centrifuge can minimize the need for conventional apparatus in the molecular diagnostic field.

To achieve a quick and high-throughput detection of disease-related biomarkers, Yang *et al.* [65] designed and 3D printed an enzyme reactor paper spray cartridge for enzyme reaction, sample transfer, and paper spray ionization (Fig. 2D). The 3D enzyme reactor cartridge was produced from autoclavable polylactic acid plastic with FDM technique. This 3D-printed cartridge coupled with mass spectrometry can evaluate butyrylcholinesterase (BuChE) activity in human serum while avoiding cumbersome sample pretreatment and tedious traditional practices. Similarly, for simplifying ELISA assays, Sharafeldin *et al.* [64] developed a new versatile diagnostic tool: ELISA in 3D-printed pipet tips, to detect four cancer biomarkers (Fig. 2E). The transparent 3D-printed pipette tips were printed by a low-cost stereolithographic printer. Compared with traditional ELISA, the new one offers a versatile and multiplexed protocol with a shorter incubation time and lower sample and reagent consumption. Besides, Lv *et al.* [62] fabricated a photoelectrochemical aptasensor with the homemade 3D printer for carcinoembryonic antigen (CEA) detection (Fig. 2F). All examples indicate that 3D printing is a promising and low-cost method for the design and manufacture of simple IVD tools.

3.1.2. Single-functional modules with sophisticated microstructure

Extensive efforts have been made to explore several types of sophisticated microstructures in the 3D-printed single-functional modules, including micropillar, microarray, micropore, microchan-

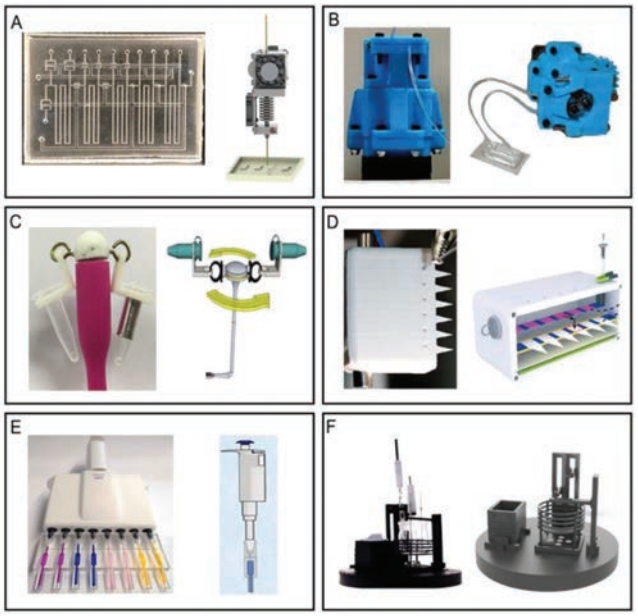

Fig. 2. (A) PDMS microfluidic chips replicated with a 3D-printed mold. Reproduced with permission [36]. Copyright 2019, American Chemical Society. (B) The 3D-printed parts assembled an open-source peristaltic pump enabling small volume liquid handling. Reproduced with permission [35]. Copyright 2020, Nature Publishing Group. (C) A minimized centrifugal system was combined with the 3D-printed rotor module for magnetic particle separation. Reproduced with permission [63]. Copyright 2019, Elsevier. (D) The 3D-printed enzyme reactor paper spray mass spectrometry cartridge. Reproduced with permission [65]. Copyright 2019, American Chemical Society. (E) The 3D-printed pipette tip. Reproduced with permission [64]. Copyright 2019, American Chemical Society. (F) Model of assembled 3D-printed photoelectrochemical device. Reproduced with permission [62]. Copyright 2020, Elsevier.

nel, microneedle, and micro-capillary. Those sophisticated microstructures have been designed and fabricated mainly for biological fluid extraction, sample capture, target recognition, and signal readout [26,28,57,66-69]. Recently, Panat *et al.* [47] reported a biosensing platform for detecting COVID-19 antibody within seconds. It consists of 3D-printed electrodes with 3D micropillars, which are coated with reduced-graphene-oxide and specific viral antigens (Fig. 3A). The micropillars used for target recognition are fabricated with Aerosol Jet printing technique. The analytical sensitivity of the biosensing platform for COVID-19 antibody detection is 2.8×10^{-15} mol/L. A novel 3D-printed microarray functionalized with epithelial cell adhesion molecule (EpCAM) antibody was exploited to capture circulating tumor cells (CTCs) from a blood sample (Fig. 3B) [57]. This 3D-printed microarray was fabricated with FDM using either photocurable resins or casting wax. The high surface area of the microarray structure is beneficial for increasing CTC capture efficiency to $>$ 90%, which is the highest value ever reported.

Besides, Balsara *et al.* [68] designed the micropore structure and coated its surface with a nanostructured block copolymer, which contained functional groups ($-SO_3^-$) to bind the administered drug (doxorubicin). The porous cylinders prepared from customized resin with a 3D printer demonstrated feasibility for measuring and modulating the dosage of drugs in routine cancer chemotherapy, thus minimizing toxic side effects (Fig. 3C). Additionally, Li *et al.* [67] fabricated a multi-material transparent microchannel structure for fluorescence detection within 40 minutes by a ROVA 3D FDM printer which is equipped with 5 extruders (Fig. 3D). The multi-functional microfluidic device was utilized for the extraction of small molecule pharmaceuticals from urine and subsequent quantification.

Traditional injection and extraction are usually subject to cumbersome operations or unbearable pain for patients. To address this issue, Yao *et al.* [28] proposed a low-cost and rapid method to fabricate hydrogel microneedles with a self-built 3D printer that can perform high-precision digital light processing (Fig. 3E). The biocompatible microneedles were successfully used for sample extraction and drug detection in ISF.

Moreover, the signal readout is also an important part of detection. The sophisticated 3D-printed capillaric circuits (3D-CC) were proposed for clinical application in resource-limited settings [37]. The 3D-CC was fabricated from acrylate photopolymer resin with an SLA-based 3D printer. The portable platform enabled rapid analysis of blood viscosity and signal readout for naked-eye, while conventional viscosity measurement depended on costly viscometers (Fig. 3F). The precision manufacturing feature of 3D printing techniques guarantees the successful fabrication of the above-mentioned sophisticated microstructures, which might improve the efficiency of R&D of IVD products.

3.2. Multi-function devices

By taking advantage of layer-by-layer manufacture, 3D printing could be easily realized the fabrication of not only the sophisticated microstructures but also the integrated functional sensor devices that enable semi-automated biochemical measurements [57,69-71]. Recently, the integrated and multiplexed biosensors have achieved far advancement [39,64-67]. For example, Li *et al.* [69] demonstrated a 3D-printed dual-modal immunosensor chip that integrated all step-analysis functional modules, including immune response, separation, and detection (Fig. 4A). The fabricated microfluidic chips offered dual readouts for realizing fast quantitative colorimetric tests and photoelectrochemical quantitation of alpha-fetoprotein (AFP). In another example, a simple, disposable, and fully 3D-printed microfluidic reactor array was developed to carry out extraction, purification, and isothermal amplification of nucleic acids in various body fluids (Fig. 4B) [70]. The low-cost 3D-printed device can detect 100 fg/reaction of *P. falciparum* gDNA and 50 CFU/reaction of *N. meningitidis* bacteria in body fluids, respectively. The multi-functional molecular diagnostic device which was comparable to benchtop instruments, was printed by an inexpensive, high-definition SLA method.

Similarly, Munoz *et al.* developed a portable multi-functional analytical system using FDM technology which can manipulate microliter solutions with high precision and perform nanoliter injections with high reproducibility (relative standard deviation $<$ 3%). The 3D-printed system contains three modules: autosampler, syringe injection pump, and electrochemical detection system (Fig. 4C). Notably, the 3D-printed system was successfully demonstrated for the analysis of a seized cocaine sample spiked with paracetamol. The correlation coefficient of 0.995 and recovery value of 105% prove its feasibility and practicability for real sample analysis [71]. More importantly, 3D printing enabled the fabrication of a low-cost and multi-functional platform accessible to general chemistry labs. In addition to these, an electrochemical sensor was fully additively manufactured with FDM using various inks. The conductive electrodes (working electrodes, counter electrodes, and reference electrodes) and the non-conductive inert electrochemical cells were designed and then printed by commercial ABS and a mixture of carbon black/polylactic acid, respectively [57]. The simple and low-cost RepRap 3D-printer can produce a complete electrochemical analysis platform in-house or in an ordinary chemistry laboratory (Fig. 4D). The analytical performance of the 3D-printed sensors was proved to be better than commercial screen-printed carbon electrodes.

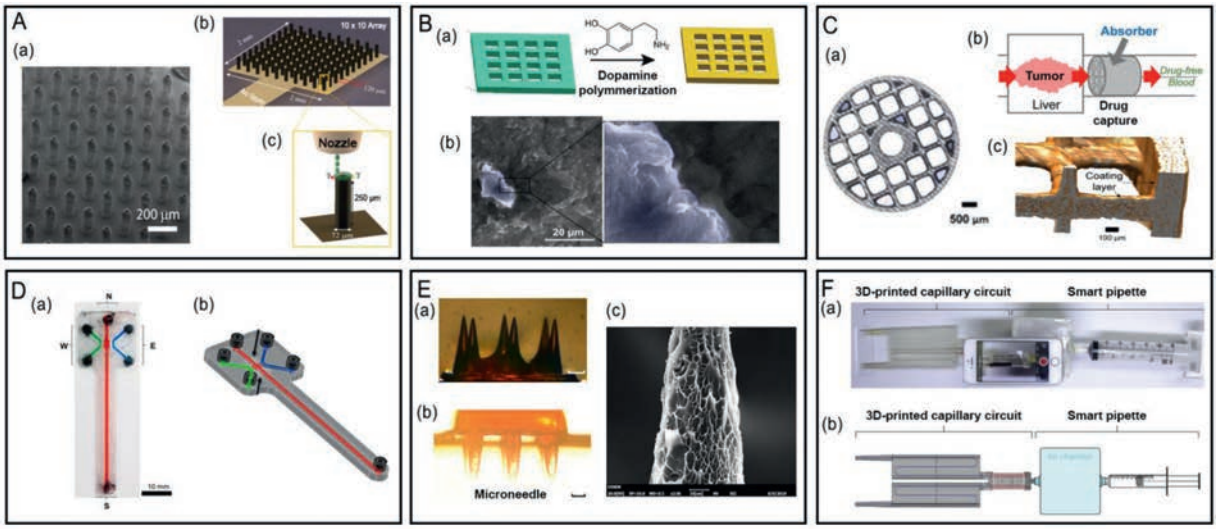

Fig. 3. (A) 3D-printed micropillar. (a) SEM of 3D micropillar, (b) image of 3D-printed 10 × 10 micropillar, and (c) details of 3D printing of a single micropillar. Reproduced with permission [47]. Copyright 2021, Wiley. (B) A 3D-printed microfluidic device was fabricated with specially designed interior (a) microarray structures to isolate CTCs from a spiked blood sample. (b) SEM images of the captured tumor cells on the 3D-printed material surface. Reproduced with permission [57]. Copyright 2020, Elsevier. (C) (a) 3D-printed porous cylinder. (b) A 3D-printed porous absorber coated with a block copolymer has a strong affinity for the chemotherapy drugs (DOX) from the bloodstream, thereby evaluating systemic toxic side effects. (c) magnified views of the 3D-printed porous cylinder. Reproduced with permission [68]. Copyright 2019, American Chemical Society. (D) 3D-printed integrated chip with multi-microchannel structure. (a) The real product and (b) a photograph of the 3D-printed chip. Reproduced with permission [67]. Copyright 2019, American Chemical Society. (E) 3D-printed hydrogel microneedles based on high precision digital light processing (H-P DLP) system and SEM of microneedle surface of tip area. Reproduced with permission [28]. Copyright 2020, Multidisciplinary Digital Publishing Institute. (F) Schematics and pictures of the 3D-printed capillary circuit for whole blood analysis. Reproduced with permission [37]. Copyright 2018, Elsevier.

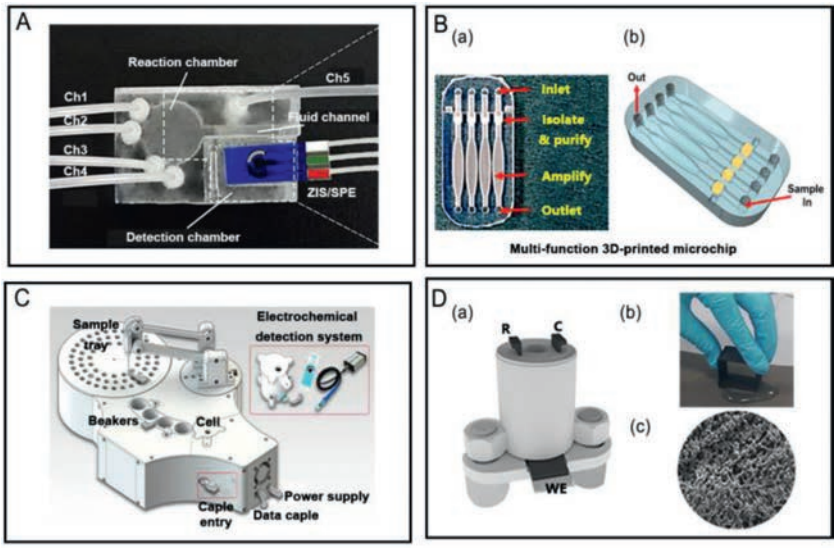

Fig. 4. (A) The 3D-printed dual-modal sensor. Reproduced with permission [69]. Copyright 2020, Elsevier. (B) (a) The multi-functional 3D-printed microchip with different function modules. (b) The design drawing of the 3D-printed microchip. Reproduced with permission [70]. Copyright 2018, Elsevier. (C) Diagram of 3D-printed parts of the analytical system. Reproduced with permission [71]. Copyright 2019, Wiley. (D) The 3D-printed electrochemical sensing platform and SEM image of the conductive electrode. Reproduced with permission [57]. Copyright 2019, American Chemical Society.

3.3. All-in-one system

Traditional laboratory-based detection methods still suffer from the operational knowledge gaps, the equipment cost, and the per-assay cost of testing reagents, especially in the resource-limited area. It is highly desirable to develop accurate and cost-effective methods implemented with easy-to-use portable devices for clinical diagnosis and healthcare monitoring in low-resource settings. Besides the fabrication of single-function modules and multi-function devices, 3D printing is also beneficial for the rapid fabrication of prototypes of all-in-one sensing systems [31,72-80]. This section will discuss 3D-printed comprehensive sensing systems with a special focus on smartphone-based chem-/bio-sensing systems.

3.3.1. Smartphone-based sensing system

The smartphone has become an appealing platform for the development of on-site quantitation instruments in low-resource settings due to the advanced computing capability, open-source operating system, and powerful built-in sensors, which can substantially simplify the instrument design and enable easy-to-use detection [81-84]. However, challenges still exist in the design and rapid fabrication of peripheral accessories for smartphone-based sensing systems. The ubiquitous 3D printing technology has cre-

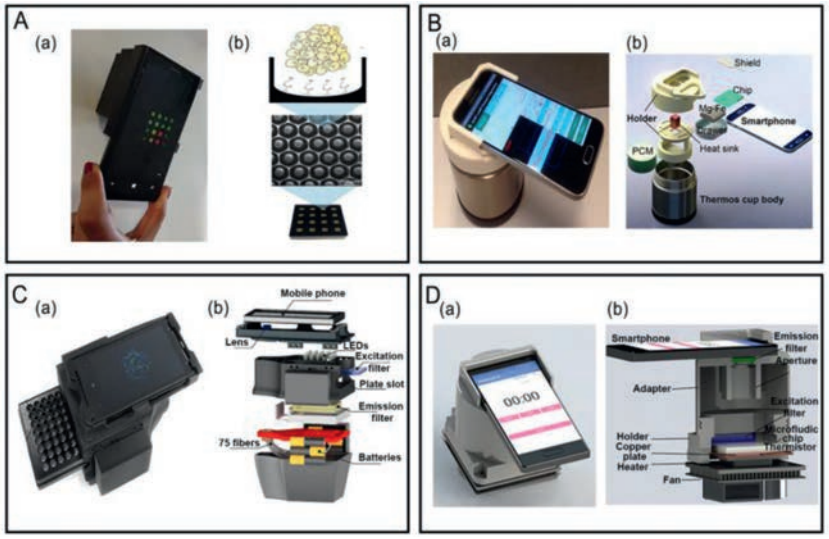

Fig. 5. (A) The smartphone-based sensing system is based on the genetically engineered bioluminescent cells and dual-color bioluminescent 3D spheroids within a 3D-printed cartridge. Reproduced with permission [81]. Copyright 2019, Elsevier. (B) The image and explosive view of the assembled smart-connected cup for mobile molecular diagnosis. Reproduced with permission [84]. Copyright 2018, American Chemical Society. (C) The image and explosive view of smartphone-based fluorescence quantification reader integrated isothermal nucleic acid assays for POC molecular diagnosis. Reproduced with permission [82]. Copyright 2017, American Chemical Society. (D) The prototype and CAD design drawing of the smartphone-based digital PCR instrument. Reproduced with permission [83]. Copyright 2018, Elsevier.

ated a golden opportunity to produce easy-to-use all-in-one systems, which substantially shortened and streamlined the development process and enhanced the practicality of the analytical devices.

A series of 3D-printed smartphone optosensing platforms have been successfully developed to integrate colorimetric [85,86] and/or fluorometric [87,88] detections with a smartphone for on-site quantitation of streptomycin, mycobacterium tuberculosis, zearalenone, and heavy metal ions. Besides, by taking advantage of 3D printing, cost-effective and rapid fabrications of smartphone-controlled electrochemical analyzers have been realized [89,90]. These prototypes, which can implement cyclic voltammetry and differential pulse voltammetry measurements, have been successfully applied for point-of-need detection of microcystin-LR and Cd^{2+}, Cu^{2+}, Hg^{2+}, Pb^{2+}, respectively.

Indeed, most IVD applications are still dominated by samples executed in the centralized laboratory, in which many analytical procedures require expensive instruments and trained professionals [24]. However, with 3D printing, the concept of smartphone-based sensing systems for IVD applications has signified a major trend over the past decade. By combining specifically designed and 3D-printed peripheral accessories, smartphone-based sensing systems can realize POCT detection inlow-resource settings. For example, a smartphone-based bioluminescent 3D whole-cell sensing system has been developed for the quantitative effect-based analysis of samples with pro- or anti-inflammatory activity [81]. All the peripheral accessories, including a cell cartridge containing 16 square wells, a black-box, a cartridge holder, and an adaptor, are fabricated with a desktop 3D printer (Makerbot Replicator 2×) by black poly(lactic acid) (PLA) and black ABS. The self-supporting device can be easily assembled by combined 3D-printed parts (Fig. 5A). HEK293 cells are genetically engineered with red- and green-emitting luciferases, serving as inflammation and viability reporters after being immobilized on the cell cartridges. The smartphone-based 3D all-in-one sensing system can detect tumor necrosis factor (TNFα) on-site with a detection limit of 0.15 ± 0.05 ng/mL.

The analysis of nucleic acids plays a crucial role in various applications such as diagnosis of infectious diseases, public health surveillance, bioprospecting, environmental conservation, and food inspection and quarantine. Therefore, extensive research efforts have focused on developing smartphone-based sensing systems for the on-site quantitation of nucleic acid in low-resource settings. For example, 3D-printed accessories, including chip holders, cup lids, and smartphone adaptors, are integrated with a smartphone and a thermos cup body with vacuum insulation for prototyping a low-cost mobile sensing system (Fig. 5B) [84]. The comprehensive sensing system relies on the combination of the bioluminescent assay in real-time and loop-mediated isothermal amplification (LAMP) technology. Of note, the 3D-printed holder established an efficient connection between the temperature control modules and the sensing modules. The successful quantitative detection of Zika virus and HIV in real samples and the generation of disease spatiotemporal mapping demonstrated the utility of the system.

A custom-designed 3D-printed optomechanical interface is integrated by Kong *et al.* with the camera module of a smartphone to assemble a portable fluorescent microplate reader (Fig. 5C) [82]. With the hydroxynaphthol blue as a chemical additive, intercalator-based fluorescence readout of nucleic acid concentration can be stabilized and significantly enhanced, allowing for the change in fluorescence to be visualized earlier and 20-fold higher than the gold standard (with a detection limit of 25 copies/μL). No baseline corrections or reference dyes to normalize results are required in the reported nucleic acid quantitation assay, simplifying the instrument design. The smartphone-based fluorescent microplate reader can easily sense this enhanced signal in a POC setting and be easily integrated with existing standard nucleic acid assays.

In addition to LAMP technology, digital polymerase chain reaction (dPCR) is also successfully integrated with smartphone-based sensing systems for quantification of nucleic acids in low-resource settings [83]. The smartphone-based dPCR system consists of a thermocycler, a microfluidic dPCR chip, optical accessories, an adapter, and a smartphone. The adapter and device holder are fabricated with 3D printing (Fig. 5D). The quantitation of the human 18 S ribosomal DNA fragment down to 10 copies and detection of single-molecule of cancer biomarker gene CD147 have proved that

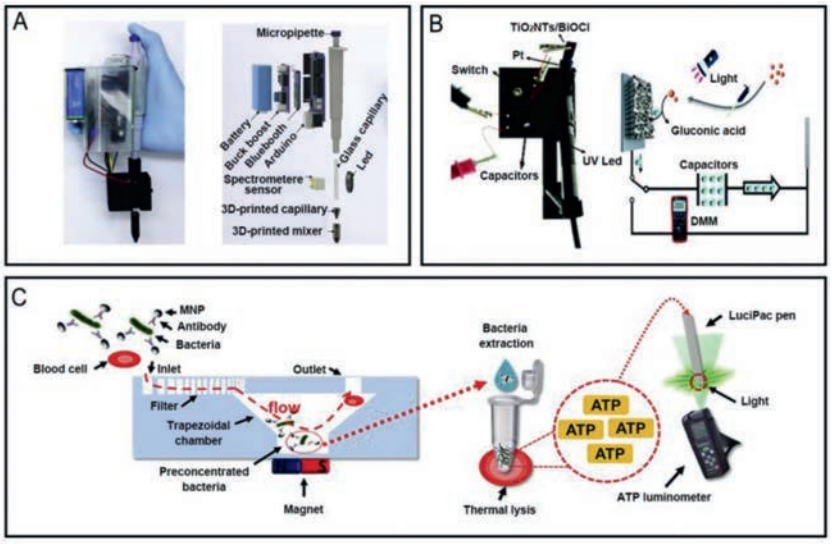

Fig. 6. (A) The wireless, portable, and open-source spectrometer for evaluating the hemolytic potential of drugs. Reproduced with permission [54]. Copyright 2020, Elsevier. (B) The portable 3D-printed PEC sensing device using a DMM for CEA detection. Reproduced with permission [93]. Copyright 2019, the Royal Society of Chemistry. (C) The 3D-printed microfluidic magnetic separation chip for specific extraction and detection of bacteria using a portable ATP luminometer. Reproduced with permission [91]. Copyright 2017, Elsevier.

the reported dPCR system is a low-cost and robust tool for highly sensitive and accurate DNA quantitative analysis.

3.3.2. Commercially available portable meters-based sensing system

The integration of commercially available handheld meters with well-developed molecular assays is an alternative strategy to develop portable all-in-one sensing systems for non-specialists conducting IVD at home or in low resource settings [38,54,91-93]. Directly making use of the existing commercially available handheld meters to the maximum extent saves financial costs for the development of a new POC device, reducing its learning curve, and increasing the odds of bringing new POCTs to reality [10]. Especially, 3D printing does help remove the intractable concerns such as sample pretreatment and optimal sensor placement. Besides, with the help of 3D printing, which exhibits the direct design-to-object workflow, the time of the R&D process can be significantly reduced.

For example, Choi *et al.* developed a portable spectrometer by assembling a broad-band light emitting diode (LED), a rectangular glass capillary, a micro electro mechanical systems (MEMS) spectrometer sensor, a fixed-volume pipette, a digital I/O board, a Bluetooth module, a buck-boost converter, an alkaline battery, a 3D-printed capillary, and a 3D-printed mixer in a 3D-printed housing (Fig. 6A) [58]. The liquid sample can be loaded into the glass capillary using the partial vacuum generated by plunger depression and release. The 3D-printed mixer enables the kinetics studies of biochemical reactions. Accurate multispectral analysis has been successfully demonstrated by assessing the hemolytic potential of Triton X-100 and studying the catalytic degradation kinetics of methylene blue. This brand-new portable spectrometer enables continuous, wireless, multispectral analysis without sample cross-contamination by non-expert users and further upgrading the design for various usage.

A commercially available digital multimeter (DMM) is successfully conditioned as a signal readout instrument for the quantitation of CEA by being integrated with a 3D-printed device [93]. The 3D-printed device consists of an L-shaped pedestal for mounting other components, a connector for connecting an ultraviolet light-emitting diode (UV LED), two detection cells, and two support brackets (one for the connector and one for UV LED) (Fig. 6B). The presence of CEA results in the formation of the sandwiched complex of the magnetic bead/aptamer 1/aptamer 2/glucose-encapsulated liposomes. The encapsulated glucose can act as the electron donor after being released, thus enhancing the photocurrent response converted to instantaneous current by the capacitor. The instantaneous current signal can be measured by a DMM. Therefore, the portable photoelectrochemical sensing system consisting of a DMM, a 3D-printed device, and a photocurrent response electrode is successfully demonstrated for CEA quantitation in low-resource settings [92].

Inspiringly, 3D printing enables the design and manufacture of sensor accessories in a very facile way. Park *et al.* [91] reported a 3D-printed microfluidic magnetic preconcentrator to collect bacterial pathogens without extra enrichment steps. The preconcentration of enterohemorrhagic *E. coli* O157:H7 in 100 mL by a factor of 700 within 1 h is successfully demonstrated. By determining adenosine triphosphate (ATP) with a commercially available ATP luminometer, the detection limit for *E. coli* O157:H7 in the blood can go down to 10 CFU/mL (Fig. 6C)

4. Commercial IVD products using 3D printing technology

The most significant advantage of adopting 3D printing in the development of IVD products is prototype and concept iteration since intensive testing is compulsory for medical products on safety grounds. In addition, 3D printing is even capable of freeform fabrication of devices with complex 3D geometries through a one-step process. In recent years, with the rapid development of 3D printing, more and more 3D-printed IVD products are becoming commercially available. In this section, a brief summary of some 3D-printed IVD products will be presented. As summarized in Fig. 7, 3D printing has penetrated into most aspects of the IVD industry and launched inspiring successes. Remarkably, more and more innovative 3D-printed IVD products are in the pipeline.

In 2020, the outbreak of COVID-19 results in a severe shortage of sampling swabs. To address this critical issue, EnvisionTEC Inc. in Dearborn developed a new production process using 3D printing for rapid production of a large number of sampling cotton swabs on the front-lines (Fig. 7A). The testing capability is substan-

Fig. 7. (A) 3D-printed sampling swabs (copyright: EnvisionTEC Inc. https://www.arabamericannews.com/2020/04/03/dearborn-based-3d-printing-company-steps-up-to-fulfill-demand-for-covid-19-testing-swabs/). (B) Examples of microfluidic chips manufactured using the Fluidic Factory 3D printer (copyright: Dolomite Inc. https://3dprint.com/124532/fluidic-factory-3d-printer/). (C) The integrated 3D-printed microfluidic device called "Vasu" for on-site malaria parasites count (copyright: Luxexcel Inc. https://3dprint.com/78793/tudelft-luxexcel-student-award/). (D) The 3D-printed blood test instrument called "Miriam" for multiplexed microRNA detection on-site (copyright: Miroculus Corp. https://tigertranscript.com/4472/health/a-miroculus-invention/). (E) The 3D-printed miniature sperm testing instrument for male infertility evaluation on-site (copyright: Harvard-affiliated Brigham and Women's Hospital. https://consumer.healthday.com/infertility-information-22/infertility-news-412/smartphone-device-sizes-up-sperm-health-720902.html).

tially enhanced by manufacturing sampling swabs *in situ*, giving the public more confidence in defeating the sustained catastrophe of COVID-19.

Dolomite Inc., a leading supplier of microfluidics, has unveiled its Fluidic Factory 3D printer, the first commercially available 3D printer for quick and easy fabrication of sealed microfluidic chips. The microfluidic functional modules such as valves, connectors, fluid manifolds, and integrated microfluidic chips (Fig. 7B) can be fabricated using FDA-approved cyclic olefin copolymer (COC) materials which is biocompatible and translucent. Due to its exceptional clarity, high purity, and inert nature, COC prevents possible interference during the reactions and analysis. Therefore, the 3D-printed functional modules and the microfluidic chips will be suitable for IVD applications.

Luxexecel Inc. is well-known for its optical 3D printing, capable of creating highly accurate, smooth, and transparent optical components. A microfluidic device, "Vasu", one of the 2015 luxexecel innovation and Application Award winners, is designed for malaria diagnosis and fabricated using optical 3D printing (Fig. 7C). With the assistance of a smartphone installed with the customized App, the instrument can analyze the images and quantify the number of malaria parasites on-site. Although the "Vasu" device is not yet a commercially viable product, its design principle can be easily transplanted to the detection of other biomarkers, making the on-site diagnosis in resource-limited areas possible.

The laboratory-based diagnosis methods still require cumbersome sample pretreatment, expensive instruments, and professional technicians. Low-cost and portable sensing systems are highly desirable for the IVD industry. Again, 3D printing significantly contributes to the manufacture of semi-automated or automated sensing systems. For example, Miroculus, a medical device start-up, has developed an accurate blood test instrument called "Miriam" for early cancer diagnosis (Fig. 7D). A proprietary 3D-printed test plate was used to detect and analyze specific microRNAs with only 1.0 mL blood sample within 1 h. With the assistance of digital microfluidic technology and an open-source artificial intelligence tool software, Miriam enables non-professionals to intervene and automatically complete the whole process from sample loading to test result reports. More importantly, 3D printing makes Miriam cheap to be manufactured.

In another successful example, 3D printing is employed to manufacture a fully automated, all-in-one sperm test instrument (Fig. 7E). By simply connecting the device to a smartphone installed with the customized app, semen samples can be easily measured to assess the fertility by non-professionals at home. Most of the components of the tiny sperm testing instrument, such as optical attachment and disposable microchip, are fabricated by 3D printing, so the total cost and weight of the instrument are only \$4.45 and ~20 g per set, respectively. Moreover, it takes less than 5 s to obtain the sperm count and assess their ability to swim with 98% accuracy. This verifies the cost-effectiveness, portability, and practicability of the 3D-printed sperm test instrument for on-site fertility evaluation.

In short, the above-mentioned portable sensing systems are inspiring examples of the application of 3D printing in the IVD industry. Undoubtedly, 3D printing facilitates the translation of IVD from centralized labs to POCT, and further bridges the gap between academia and the industrial community.

5. Conclusions and outlooks of 3D printing in the field of IVD

The past decade witnessed the dramatic development of 3D printing technology. In this paper, the typical 3D printing techniques and the corresponding manufacturing processes were systematically summarized and reviewed with emphasis on SLA, DLP, FDM, and inkjet printing that have been widely adopted in IVD field. Owing to the outstanding capability in rapid fabrication and iterative design, 3D printing has facilitated the IVD industry in terms of materials, devices, and system integration. Specifically, simple 3D-printed IVD tools and multi-functional devices have boosted the transformation of IVD from central labs to POCT in resource-limited settings. More importantly, 3D printing plays an important role in bridging the gap between research prototypes and industrial products, eventually empowering the rapid deployment of innovative IVD products. Though the enormous advantages are clearly manifested, the fabrication of 3D-printed IVD products is still in its infancy, and several critical issues concerning the current and future practical applications in IVD field need to be addressed. Therefore, the following prospects of 3D printing are highly anticipated for IVD applications.

5.1. High-performance 3D printing techniques

A typical diagnostic assay always involves multiple analytical procedures such as sample pretreatment, target capture, recognition, and quantitation. For a practical and ideal diagnostic assay, different procedures require different materials with different machining precision. Though typical 3D printing techniques such as SLA, DLP, FDM, and inkjet printing have made IVD products more practical, more accurate, and more functional than before, the issues of low-efficiency and low-resolution still exist. The 3D printing techniques capable of processing multiple materials are beneficial for efficiently elaborating IVD devices with multiple functions. Meanwhile, 3D printing techniques with improved resolutions are beneficial to fabricate microstructure with improved pre-

cision and significantly improve the analytical performance of IVD products. Therefore, high-performance 3D printing techniques capable of processing multiple materials with significantly improved resolutions are becoming a research hot spot.

5.2. Fully integrated all-in-one 3D-printed devices

Recently, integrated and miniaturized analytical devices have increasingly attracted research attention. Fully integrated all-in-one 3D-printed devices would tremendously improve the analytical performance by simplifying the detection process. For example, step-by-step assays may significantly increase reagent consumption and the risks of sample contamination. However, taking advantage of the automatic operation design, those potential error-generating steps such as reagent introduction, sample mixing, and analyte detection may be eliminated with fully integrated 3D-printed devices. Undoubtedly, all-in-one 3D-printed sensing systems achieve rapid detection in a low-cost and highly efficient manner, which satisfies the requirements of POCT applications. With the help of 3D printing, the development process of easy-to-use all-in-one sensing systems tends to be simplified. Constant research efforts in designing and prototyping the fully integrated all-in-one 3D-printed analytical devices are essential for future IVD development.

5.3. 3D-printed smartphone-based sensing systems

Smartphones have presented themselves as an appealing platform for the development of easy-to-use sensing systems for POCT applications. The powerful built-in sensors, advanced computing capability, and open-source operating systems of smartphones eliminate the need for additional detectors and laptop computers during data processing. Smartphones could facilitate on-site quantitation in low-resource settings by simplifying the instrument design and enabling easy-to-use detection. Therefore, by combining specifically designed peripheral accessories and adequately designed software, smartphones can be conditioned as all-in-one sensing systems for various IVD applications. The 3D printing technology can also substantially shorten and streamline the prototyping of smartphone-based sensing systems. Continuous research efforts should be directed to developing smart 3D-printed sensing systems for nascent IVD applications.

Declaration of competing interest

The authors declare no conflict of interests.

Acknowledgments

This research is financially supported by the National Natural Science Foundation of China (No. 51975597), the Guangdong Natural Science Foundation (No. 2020A1515010661), the Science and Technology Project of Guangzhou (No. 201803020026), the General Program of Shenzhen Innovation Funding (Nos. JCYJ20170818164246179 and JCYJ20170307140752183), and the Fundamental Research Funds for the Central Universities (No. 20lgzd27).

References

[1] C.L.M. Palenzuela, M. Pumera, TrAC Trends Anal. Chem. 103 (2018) 110–118.
[2] Y. Wang, Y.S. Xia, Microchim. Acta 186 (2019) 50.
[3] A. Bolotsky, D. Butler, C.Y. Dong, K. Gerace, et al., ACS Nano 13 (2019) 9781–9810.
[4] Z. Xi, H.H. Ye, X.H. Xia, Chem. Mater. 30 (2018) 8391–8414.
[5] X.Y. Cui, L. Cao, Y.L. Huang, et al., Analyst 143 (2018) 3011–3020.
[6] S. Nisiat, F.R. Awan, S.Z. Bajwa, Anal. Sci. 35 (2018) 123–131.
[7] R. Haldavnekar, K. Venkatakrishnan, B. Tan, Nat. Commun. 9 (2018) 3065.
[8] J. Shin, S. Chakravarty, W. Choi, et al., Analyst 143 (2018) 1515–1525.
[9] V. Gupta, P. Mahbub, P.N. Nesterenko, B. Paull, Anal. Chim. Acta 1005 (2018) 81–92.
[10] M. Wu, Q. Lai, Q. Ju, et al., Biosens. Bioelectron. 102 (2018) 256–266.
[11] M.R. Khosravani, T. Reinicke, Sens. Actuators A 305 (2020) 111916.
[12] S. Pravin, A. Sudhir, Biomed. Pharmacother. 107 (2018) 146–154.
[13] A. Lambert, S. Valiulis, Q. Cheng, ACS Sens. 3 (2018) 2475–2491.
[14] G.W. Bishop, J.E. Satterwhite-Warden, K. Kadimisetty, J.F. Rusling, Nanotechnology 27 (2016) 284002.
[15] D.J. Cocovi-Solberg, P.J. Worsfold, M. Miró, TrAC Trends Anal. Chem. 108 (2018) 13–22.
[16] F. Li, M.R. Ceballos, S.K. Balavandy, et al., J. Sep. Sci. 43 (2020) 1854–1866.
[17] H.N. Chan, M.J.A. Tan, H.K. Wu, Lab Chip 17 (2017) 2713–2739.
[18] Y. Zhang, S.G. Ge, J.H. Yu, TrAC Trends Anal. Chem. 85 (2016) 166–180.
[19] D.J. Cocovi-Solberg, M. Rosende, M. Michalec, M. Miro, Anal. Chem. 91 (2019) 1140–1149.
[20] E.J. Carrasco-Correa, E.F. Simó-Alfonso, J.M. Herrero-Martínez, M. Miró, TrAC Trends Anal. Chem. 136 (2021) 116177.
[21] R.M. Cardoso, C. Kalinke, R.G. Rocha, et al., Anal. Chim. Acta 1118 (2020) 73–91.
[22] M. Grajewski, M. Hermann, R.D. Oleschuk, E. Verpoorte, G.I. Salentijn, Anal. Chim. Acta 1116 (2021) 338332.
[23] G.I.J. Salentijn, P.E. Oomen, M. Grajewski, E. Verpoorte, Anal. Chem. 89 (2017) 7053–7061.
[24] J.J. Zhang, T. Lan, Y. Lu, TrAC Trends Anal. Chem. 124 (2020) 115782.
[25] R.A. Mendoza, A. Rios, J.L. Garcia-Cordero, Anal. Chem. 90 (2018) 5563–5568.
[26] R.K. Gao, X. Tian, Q.Z. Li, et al., Chem. Mater. 32 (2020) 3188–3198.
[27] H.G. Yi, Y.H. Jeong, Y. Kim, et al., Nat. Biomed. Eng. 3 (2019) 509–519.
[28] W. Yao, D.D. Li, Y.L. Zhao, et al., Micromachines 11 (2019) 17.
[29] K. Zhang, S. Lv, D. Tang, Anal. Chem. 91 (2019) 10049–10055.
[30] K. Kadimisetty, S. Malla, K.S. Bhalerao, et al., Anal. Chem. 90 (2018) 7569–7577.
[31] G. Papadakis, A.K. Pantazis, M. Ntogka, et al., ACS Sens. 4 (2019) 1329–1336.
[32] H. Motaghi, S. Ziyaee, M.A. Mehrgardi, A.A. Kajani, A.K. Bordbar, Biosens. Bioelectron. 118 (2018) 217–223.
[33] G. Scordo, D. Moscone, G. Palleschi, F. Arduini, Sens. Actuators B 258 (2018) 1015–1021.
[34] N.C. de Moraes, E.N.T. da Silva, J.M. Petroni, V.S. Ferreira, B.G. Lucca, Electrophoresis 41 (2020) 278–286.
[35] M.R. Behrens, H.C. Fuller, E.R. Swist, et al., Sci. Rep. 10 (2020) 1543.
[36] B.V. Dang, A. Hassanzadeh-Barforoushi, M.S. Syed, et al., ACS Sens. 4 (2019) 2181–2189.
[37] S. Oh, B. Kim, J.K. Lee, S. Choi, Sens. Actuators B 259 (2018) 106–113.
[38] R.M. Dirkzwager, S.L. Liang, J.A. Tanner, ACS Sens. 1 (2016) 420–426.
[39] R.M. Cardoso, P.R.L. Silva, A.P. Lima, et al., Sens. Actuators B 307 (2020) 127621.
[40] S. Stassi, E. Fantino, R. Calmo, et al., ACS Appl. Mater. Interfaces 9 (2017) 19193–19201.
[41] A. Abdalla, B.A. Patel, Curr. Opin. Electrochem. 20 (2020) 78–81.
[42] X. Fu, B. Xia, B.C. Ji, S. Lei, Y. Zhou, Anal. Chim. Acta (2019) 64–70.
[43] S.M. Feng, D.D. Liu, G.Q. Feng, Anal. Chim. Acta 1054 (2019) 137–144.
[44] F. Cecil, R.M. Guijt, A.D. Henderson, M. Macka, M.C. Breadmore, Anal. Chim. Acta 1097 (2019) 127–134.
[45] W.Q. Chang, J.L. Zhou, Y. Li, Z.Q. Shi, G.Z. Xin, Anal. Chim. Acta 950 (2016) 138–146.
[46] E.C. Sweet, N. Liu, J. Chen, L. Lin, IEEE 32nd Int. Conf. Micro Electro Mech. Syst, (MEMS), 2019, pp. 79–82.
[47] C.H. Ali, S. Jahan, B Yuan, et al., Adv. Mater. 33 (2021) 2006647.
[48] X.J. Chen, H. Chen, D.Z. Wu, et al., Sens. Actuators B 276 (2018) 507–516.
[49] K. Shigeta, Y. He, E. Sutanto, et al., Anal. Chem. 84 (2012) 10012–10018.
[50] X. Liu, W. Zheng, X. Jiang, ACS Sens. 4 (2019) 1465–1475.
[51] Y. Ding, J. Li, W. Xiao, et al., Anal. Chem. 87 (2015) 10166–10171.
[52] D. Rabha, A. Sarmah, P. Nath, J. Microsc. 276 (2019) 13–20.
[53] E.M. Richter, D.P. Rocha, R.M. Cardoso, et al., Anal. Chem. 91 (2019) 12844–12851.
[54] B. Kim, M. Jeon, Y.J. Kim, S. Choi, Sens. Actuators B 306 (2020) 127537.
[55] Y.D.H. Park, H.V. Kim, J Lee, H.C. Yoon, S. Park, Lab Chip 18 (2018) 1533–1538.
[56] V. Katseli, A. Economou, C. Kokkinos, Talanta 208 (2020) 120388.
[57] J.H. Chen, C.Y. Liu, X.C. Wang, et al., Biosens. Bioelectron. 150 (2020) 111900.
[58] F. Li, N.P. Macdonald, R.M. Guijt, M.C. Breadmore, Lab Chip 19 (2018) 35–49.
[59] L. Siebert, O. Lupan, M. Mirabelli, et al., ACS Appl. Mater. Interfaces 11 (2019) 25508–25515.
[60] S. Guo, X. Lin, Y. Wang, X. Gong, Chin. Med. 14 (2019) 13.
[61] G. Weisgrab, A. Ovsionikov, P.F. Costa, Adv. Mater. Technol. 4 (2019) 1900275.
[62] S.Z. Lv, K.Y. Zhang, Q. Zhou, D.P. Tang, Sens. Actuators B 310 (2020) 127874.
[63] Y.M. Park, C.H. Kim, S.J. Lee, M.K. Lee, Biosens. Bioelectron. 141 (2019) 111415.
[64] M. Sharafeldin, K. Kadimisetty, K.R. Bhalerao, et al., Anal. Chem. 91 (2019) 7394–7402.
[65] Y.M. Yang, H.M. Liu, Z.Z. Chen, et al., Anal. Chem. 91 (2019) 12874–12881.
[66] A. Bayram, M. Serhatlioglu, B. Ortac, et al., Sens. Actuators A 269 (2018) 382–387.
[67] F. Li, N.P. Macdonald, R.M. Guijt, M.C. Breadmore, Anal. Chem. 91 (2019) 1758–1763.
[68] H.J. Oh, M.S. Aboian, M.Y.J. Yi, et al., ACS Cent. Sci. 5 (2019) 419–427.
[69] X. Li, X.M. Pan, J.M. Lu, Y.P. Zhou, J.M. Gong, Biosens. Bioelectron. 158 (2020) 112158.
[70] K. Kadimisetty, J.Z. Song, A.M. Doto, et al., Biosens. Bioelectron. 109 (2018) 156–163.
[71] D.M.H. Mendonça, D.P. Rocha, R.M. Cardoso, et al., Electroanalysis 31 (2019) 771–777.

[72] J. Shin, S. Chakravarty, W. Choi, et al., Analyst 143 (2018) 1515–1525.
[73] H. Xu, A. Xia, J. Luo, et al., Sens. Actuators B 308 (2020) 127750.
[74] A. Malekjahani, S. Sindhwani, A.M. Syed, W.C.W. Chan, Acc. Chem. Res. 52 (2019) 2406–2414.
[75] L. Coudron, M.B. McDonnell, I. Munro, et al., Biosens. Bioelectron. 128 (2019) 52–60.
[76] C.R. Phaneuf, B. Mangadu, H.M. Tran, et al., Biosens. Bioelectron. 120 (2018) 93–101.
[77] L.J. Wang, Y.C. Chang, R.R. Sun, L. Li, Biosens. Bioelectron. 87 (2017) 686–692.
[78] Y. Jia, H. Dong, J. Zheng, H. Sun, Biomicrofluidics 11 (2017) 064101.
[79] N. Cheng, Y. Song, M.M.A. Zeinhom, et al., ACS Appl. Mater. Interfaces 9 (2017) 40671–40680.
[80] A. Roda, M. Guardigli, D. Calabria, et al., Analyst 139 (2014) 6494–6501.
[81] E. Michelini, M.M. Calabretta, L. Cevenini, et al., Biosens. Bioelectron. 123 (2019) 269–277.
[82] J.E. Kong, Q.S. Wei, D. Tseng, et al., ACS Nano 11 (2017) 2934–2943.
[83] T. Gou, J.M. Hu, W.S. Wu, et al., Biosens. Bioelectron. 120 (2018) 144–152.
[84] J.Z. Song, V. Pandian, M.G. Mauk, et al., Anal. Chem. 90 (2018) 4823–4831.
[85] X.M. Li, J. Wang, C.Q. Yi, et al., Sens. Actuators B 290 (2019) 170–179.
[86] L. Li, Z.G. Liu, H. Zhang, et al., Sens. Actuators B 254 (2018) 337–346.
[87] M. Xiao, Z.G. Liu, N.X. Xu, et al., ACS Sens. 5 (2020) 870–878.
[88] Z.G. Liu, Y.L. Zhang, S.J. Xu, et al., Anal. Chim. Acta 966 (2017) 81–89.
[89] T. Guan, W.Z. Huang, N.X. Xu, et al., Sens. Actuators B 294 (2019) 132–140.
[90] Z.Z. Xu, Z.J. Liu, M. Xiao, L.L. Jiang, C.Q. Yi, Chem. Eng. J. 394 (2020) 124966.
[91] C. Park, J. Lee, Y. Kim, et al., J. Microbiol. Methods 132 (2017) 128–133.
[92] C.W. Pinger, A. Castiaux, S. Speed, D.M. Spence, J. Chem. Educ. 95 (2018) 1662–1667.
[93] K.Y. Zhang, S.Z. Lv, D.P. Tang, Analyst 144 (2019) 5389–5393.